

Decaying Dark Matter and the Deficit of Dwarf Haloes

Majd Abdelqader¹* and Fulvio Melia²†

¹ *Department of Physics, The University of Arizona, Tucson, Arizona 85721, USA*

² *Department of Physics and Steward Observatory, The University of Arizona, Tucson, Arizona 85721, USA*

Submitted to MNRAS 2008 January 23

ABSTRACT

The hierarchical clustering inherent in Λ -CDM cosmology seems to produce many of the observed characteristics of large-scale structure. But some glaring problems still remain, including the over-prediction (by a factor 10) of the number of dwarf galaxies within the virialized population of the local group. Several secondary effects have already been proposed to resolve this problem. It is still not clear, however, whether the principal solution rests with astrophysical processes, such as early feedback from supernovae, or possibly with as yet undetermined properties of the dark matter itself. In this paper, we carry out a detailed calculation of the dwarf halo evolution incorporating the effects of a hypothesized dark-matter decay, $D \rightarrow D' + l$, where D is the unstable particle, D' is the more massive daughter particle and l is the other, lighter (or possibly massless) daughter particle. This process preferentially heats the smaller haloes, expanding them during their evolution and reducing their present-day circular velocity. We find that this mechanism can account very well for the factor 4 deficit in the observed number of systems with velocity 10–20 km s⁻¹ compared to those predicted by the numerical simulations, if $\Delta m/m_{D'} \sim 5 - 7 \times 10^{-5}$, where Δm is the mass difference between the initial and final states. The corresponding lifetime τ cannot be longer than ~ 30 Gyr, but may be as short as just a few Gyr.

Key words: cosmic microwave background—cosmology: theory—dark matter—elementary particles—galaxies: formation—large-scale structure of the universe

* E-mail: majd@physics.arizona.edu

† Sir Thomas Lyle Fellow and Miegunyah Fellow, E-mail: melia@as.arizona.edu

1 INTRODUCTION

Observations of the cosmic microwave background (CMB) radiation with the Wilkinson Microwave Anisotropy Probe (WMAP) have facilitated the precision measurement of several cosmological parameters (Bennett et al. 2003, Spergel et al. 2003), including the mass-energy density of the Universe, Ω , which appears to be close (if not equal) to its critical value. Baryons contribute only about 4% of this; the rest is presumably in the form of dark matter (DM; roughly 22%) and dark energy ($\sim 74\%$). In addition, WMAP's detection of early reionization also rules out the presence of a warm DM, so the non-baryonic component must be cold (CDM). Together with earlier observations by other finer scale CMB experiments, and with the Hubble Key Project (Mould et al. 2000), which provided the unprecedentedly accurate value $H = 71 \pm 6 \text{ km s}^{-1}$ of the Hubble constant, this combined body of work has led to a consensus that the Universe is adequately described by the so-called flat Λ -CDM standard model, in which dark energy is the manifestation of a cosmological constant Λ .

The existence of dark energy has been confirmed through the analysis of Type Ia supernova data (Riess et al. 1998; Perlmutter et al. 1999), providing even stronger evidence that this component of Ω has negative pressure leading to an acceleration of the Universe in the current epoch. To be fair, however, it is not yet entirely clear whether these results require a cosmology with a true cosmological constant, in which matter and radiation become dominant looking back towards redshifts $z > 2-3$, or whether the current acceleration might be due to a so-called scaling solution, in which the dark energy density scales with matter, and affects the formation of structure even at early times (see Melia 2007, 2008, and references cited therein).

Very little is known about dark matter, and almost nothing is understood about dark energy. Their nature is one of the biggest mysteries in contemporary physics. Yet their influence is evidently quite important in the formation of large scale structure (LSS). The hierarchical clustering inherent in Λ -CDM seems to produce many of the characteristics observed in the local (e.g., Murali et al. 2002; Abadi et al. 2003) and high-redshift (e.g., Springel, Frenk, and White 2006) Universe. In hierarchical models, smaller dark matter haloes on average collapse earlier than larger ones, when the density of the universe was higher (e.g., Kravtsov et al. 1998). The current mass function, however, is determined not only by the halo formation history, but also by their merger rate which, over time, tends to deplete the dwarf-galaxy end of the distribution.

But some glaring problems still remain. Numerical simulations involving collisionless CDM predict dark haloes with steep cusps in their centre (Navarro et al. 1996), whereas most of the

observed rotation curves of dwarf galaxies and low surface brightness galaxies indicate constant density cores (see de Blok et al. 2003, and references cited therein). A related problem is the over-prediction of the number of dwarf galaxies within the virialized population of the local group. CDM simulations over-predict the number of satellite galaxies orbiting a Milky Way-sized galaxy by a factor of 10 (Klypin et al. 1999, Moore et al. 1999, Diemand et al. 2007, and Simon & Geha 2007). Generally speaking, both of these problems may be described as a Λ -CDM prediction of too much power on small scales.

Since in hierarchical models smaller galaxies merge to make larger ones, the number of remaining dwarf haloes is an important diagnostic to test both the hierarchical picture and the process of halo condensation in the evolving universe. Thus, the dwarf-halo deficit may be taken as an indicator of new physics associated with dark matter (and/or dark energy). For example, the small-scale power can be reduced by substituting warm dark matter for CDM. But as we have seen, WMAP observations have already ruled this possibility out.

Other simple attempts to fix the dwarf-halo deficit problem are not well motivated physically. Some involve altering the fundamental nature of dark matter by introducing self-interaction, or annihilation (see, e.g., Spergel and Steinhardt 2000; Kaplinghat, Knox, and Turner 2000; and Giraud 2001, among others). Without a proper indication from physical considerations, all of these models contain free parameters tunable to fit the observations. For example, the self-interacting dark matter scenario rests on the viability of a huge velocity-dependent cross section. Unfortunately, the implied large interaction rate is inconsistent with most weakly interacting, massive particle and axion theories (see, e.g., Hennawi and Ostriker 2002).

Of course, the dwarf-halo deficit may be due to reasons other than DM physics. Many of them may be invisible because they contain a very small amount of luminous matter, either because of early feedback from supernovae (Dekel and Silk 1986; Mac Low and Ferrara 1999), or because their baryonic gas was heated by the intergalactic ionizing background radiation (Rees 1986; Barkana and Loeb 1999). Others may have turned into high-velocity clouds in the Local Group (see, e.g., Blitz et al. 1999). The deficit may not even be real if the Universe is actually older than its current inferred age, which in reality is only the light-travel time to the cosmic horizon rather than the Big Bang (Melia 2007, 2008). In such a scenario, the dwarf haloes would have had more time to merge, depleting the lower end of the mass function and bringing it into better alignment with the observations.

In any case, it is still too early to tell whether or not the discrepancy between the cosmological simulations and observations really indicates a major problem for hierarchical models in Λ -CDM.

Several of the effects we have listed here may resolve at least part of the deficit problem. However, given that this is still an open question, observations of the halo mass function also allow us to explore non-astrophysical reasons for the discrepancy, with the goal of learning more about the nature of dark matter.

Our focus in this paper is the suggestion that DM particles may be unstable to decay (see, e.g., Davis et al. 1981; Turner et al. 1984; Turner 1985; Dicus and Teplitz 1986; Dekel and Piran 1987; Sciama 1990; Cen 2001a; Sánchez-Salcedo 2003). The impact of the interactions we describe above and/or decays is almost always to provide a mass-dependent expansion of the cusps and haloes to lower the core density and to reduce the number of small galaxies. However, attempts to couple these ideas to particle physics have been few and ambiguous, partly because these have been concerned more with global effects, rather than aimed at finding specific particle properties that may be consistent with the requirements to fix the problem. Our goal in this paper is to begin a more careful search for the properties DM particles must have in order to account for the deficit of dwarf haloes, if in the end their decay is indeed responsible for the observed effect.

Our approach here is closest in spirit to the work of Cen (2001a) and Sánchez-Salcedo (2003), though their papers had different goals. Cen's (2001a) primary interest was to demonstrate that if DM particles decay and become relativistic, they escape the virialized halo, whose remaining energy then exceeds that required to sustain virial equilibrium and forces it to expand. His suggestion was that the overproduction of dwarf haloes may be solved not by removing them, but by modifying them into failed, dark galaxies, in which star formation has been quenched due to the effects of evaporation and expansion. This is an intriguing idea, though not yet sufficiently developed to provide a useful probe into the properties of the particles themselves.

Sánchez-Salcedo's (2003) goal was to mitigate the disparity between the very steep central cusps in dark haloes of dwarf galaxies predicted by Λ -CDM and the relatively flat distributions actually seen in these systems. He demonstrated that if DM decays into a relativistic, nonradiative light particle, plus a stable massive particle with some recoil velocity in the center-of-mass frame, the former escapes the bound system while the latter remains with an energy exceeding that of the parent, forcing the halo to expand.

In this paper, we introduce several new aspects of the DM-decay scenario, including the time-dependent and mass-dependent halo formation and hierarchical-merger rates in order to more accurately gauge the impact of heating on the present-day circular velocity distribution. There are too many aspects of the DM decay to consider in just one set of calculations, so we here restrict our attention to cases in which at least one of the decay products remains within the halo, maintaining

its mass, though heating it with the liberated energy. Other regions of the DM particle phase space will be explored elsewhere.

In the next section, we summarize the circular-velocity data and demonstrate the nature of the dwarf-halo deficit problem. Then in §3 we describe a technique for following the mass-dependent formation and destruction of haloes as the universe evolves. In §4 we describe the DM-particle decays and how we incorporate the impact of this process into our calculational algorithm. We present the results of our calculations in §5, and discuss them in §6.

2 THE OBSERVED CIRCULAR-VELOCITY DISTRIBUTION OF DWARF HALOES

The dwarf-galaxy deficit was first quantified when the observed number of dwarf galaxies in the local group was compared to high-resolution cosmological simulations of Klypin et al. (1999) and Moore et al. (1999), under the reasonable assumption that the local group is an adequate representation of what is happening throughout the cosmos. If we assume that each small dark matter halo contains a dwarf galaxy, then there is a substantial discrepancy between theory and observation. At the time of these simulations, there were only 13 known satellites of The Galaxy, while both simulations predicted roughly 10 times that number of satellites for a Milky Way-sized halo (Klypin et al. 1999, and Moore et al. 1999).

In the last several years, the number of pertinent observations has increased substantially, and new cosmological simulations have been completed with substantially higher resolution than the original calculations. The Sloan Digital Sky Survey (SDSS hereafter) has uncovered 10 more Milky Way companions (Belokurov et al. 2007). The discrepancy between the latest observations and the most recent simulations still exists, however, and it appears to be a function of mass. In the range of primary relevance to this paper (i.e., 10–20 km s⁻¹), the disparity is a factor 4 when compared to the latest high resolution N-body simulation known as Via Lactea (Diemand et al. 2007), even after weighting the new dwarf galaxies by a factor of 5 to account for the limited coverage of the SDSS; at 6 km s⁻¹, the discrepancy increases to a factor 10 (Simon & Geha 2007).

3 FORMATION OF BOUND OBJECTS IN THE HIERARCHICAL CLUSTERING SCENARIO

For reasons that will soon become apparent, the impact of decaying dark matter on the evolution of haloes depends on their formation history. For simplicity, we here use a semi-analytical approach that describes the halo formation rate as a function of mass and time, optimized to reproduce

numerical simulations of structure formation. A good starting point is the Press-Schechter mass function (hereafter PS), or one of its modified forms, which is a reasonable representation of the overall halo distribution resulting from these numerical simulations (Press and Schechter 1974). However, PS is a number density that combines both the formation and merger histories of the haloes, so it does not provide their formation rate explicitly. None the less, a formation rate can be extracted from the PS formalism by taking the comoving time derivative of the mass function, identifying the term corresponding to the formation rate, and multiplying it by the survivability probability. This procedure subtracts the halo destruction rate, and is necessary for our purpose since we only want to consider haloes that formed in the past and survived to the present without merging with others to form even bigger structures (see, e.g., Sasaki 1994; Kitayama & Suto 1996). The formation rate can be written as (Sasaki 1994)

$$\dot{N}_{form}(M, t) dM dt = \frac{1}{a(t)} \frac{da(t)}{dt} N_{PS}(M, t) \frac{\delta_c^2(t)}{\sigma^2(M)} dM dt, \quad (1)$$

where M is the mass of the formed gravitational structure, t is the formation time measured in comoving coordinates starting from zero at the Big Bang, $a(t)$ is the cosmological scale factor normalized to unity at the present epoch t_0 , $N_{PS}(M, t)$ is the Press-Schechter mass function, $\delta_c(t) = \frac{\delta_c}{a(t)}$ is the critical density threshold for a spherical perturbation to collapse by time t ($\delta_c \simeq 1.69$ for $\Omega_0 = 1$), and $\sigma(M)$ is the rms density fluctuation smoothed over a region of mass M . However, we are interested in haloes surviving to the present epoch, thus the above formation rate function must be multiplied by the probability $p(t_1, t_2)$ that an object which exists at t_1 remains at t_2 without merging, which is given by $p(t_1, t_2) = a(t_1)/a(t_2)$ (Sasaki 1994). The formation rate distribution of surviving haloes at the present epoch becomes $F(M, t) dM dt = \dot{N}_{form}(M, t) \times p(t, t_0) dM dt$, which can be written explicitly as

$$F(M, t) dM dt = A \frac{da(t)}{dt} \frac{1}{a(t)^3} M^{(n-1)/2} \exp \left[-\frac{1}{2} \left(\frac{M}{M_{c,0}} \right)^{(n+3)/3} \frac{1}{a(t)^2} \right], \quad (2)$$

where A is a normalization constant, n is the power-law spectral index chosen to be -2.5 , following Klypin et al. (1999), and $M_{c,0}$ is the present mass scale of the knee taken to be $10^{15} M_\odot$.

In this paper, we adopt a flat universe $\Omega_0 = 1$, represented roughly as $\Omega_{m,0} = 0.3$, and $\Omega_{\Lambda,0} = 0.7$, which gives $a(t) = (0.3/0.7)^{1/3} \sinh^{2/3}(1.21 [t/t_0])$, normalized to unity at the present epoch $t_0 = 13.7$ Gyr. Figure 1 shows the formation rate as a function of time for two illustrative halo masses. The larger mass always has the smaller formation rate, which also peaks at later times, though this difference is not very obvious from the figure as the two are relatively close.

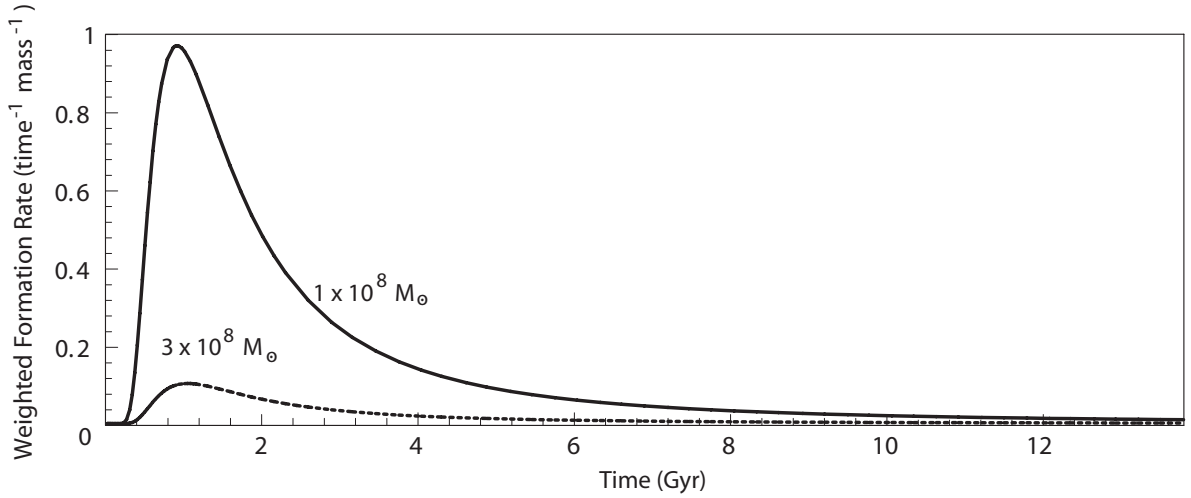


Figure 1. The relative halo formation distribution as a function of cosmic time for haloes surviving to the present epoch, for two illustrative masses: $M = 1 \times 10^8 M_\odot$ and $M = 3 \times 10^8 M_\odot$.

4 DM PARTICLE DECAYS AND THEIR IMPACT ON DWARF HALO EVOLUTION

In this paper, we focus our attention on dark matter decay scenarios in which the parent particle, denoted by D , decays into one stable massive particle (D') with a mass close to that of its parent, and one very light (possibly even massless) particle (ℓ), following the notation of Sánchez-Salcedo (2003). Due to the extreme mass ratio between the daughter particles, the light particle carries most of the energy released by the decay and becomes relativistic, escaping the halo. The massive daughter particle remaining in the halo has an (average) energy very close to, but slightly larger, than that of its parent, forcing the halo to expand adiabatically. Since the kinetic energy of the light particle is much larger than its rest mass, we neglect the latter. To this level of approximation, the total mass of the halo remains unaffected by the decay because $m_{D'} \approx m_D$.

The decay is represented as $D \rightarrow D' + \ell$. In the center-of-mass frame (denoted by a * superscript), i.e., in the rest frame of the parent particle D , the initial four-momentum vector before the decay is

$$p_i^* = (m_D c, \vec{0}), \quad (3)$$

and after the decay the final four-momentum is

$$p_f^* = p_{D'}^* + p_\ell^* = (\gamma_{D'}^* m_{D'} c, -\gamma_{D'}^* m_{D'} v_{D'}^*, 0, 0) + (E_\ell^*/c, E_\ell^*/c, 0, 0), \quad (4)$$

where we have put the direction of \vec{p}_ℓ^* along $+\hat{x}$, and $\vec{p}_{D'}^*$ along $-\hat{x}$.

Conservation of momentum leads to the equation

$$E_\ell^* = (m_D^2 - m_{D'}^2) c^2 / 2m_D. \quad (5)$$

To find the particle's energy E_ℓ in the halo's rest frame, we need to Lorentz boost the physical

quantities using the velocity $\vec{v} = \vec{v}_D$ and the angle θ^* between \vec{v} and \vec{p}_ℓ . This gives

$$E_\ell = \gamma_D E_\ell^* (1 + \beta_D \cos \theta^*) . \quad (6)$$

Averaging over all solid angles, we find that

$$\langle E_\ell \rangle = \frac{1}{4\pi} \int E_\ell d\Omega = \gamma_D E_\ell^* . \quad (7)$$

We next define the unitless parameter

$$\chi \equiv \frac{\Delta m}{m_{D'}} , \quad (8)$$

the ratio between the change in rest mass $\Delta m = m_D - m_{D'}$ and the mass of the heavier daughter particle D' . The energy of the lighter (relativistic) particle, averaged over all angles θ^* , becomes

$$\langle E_\ell \rangle = \gamma_D m_D \frac{\chi(2 + \chi)}{2(1 + \chi)^2} c^2 . \quad (9)$$

If both particles remain in the halo, then the change in the halo's energy for each decay is simply $\Delta m c^2$. However, the lighter particle escapes, so its energy must be subtracted. We find that for this type of decay, the rate of change in the halo's energy is therefore

$$\frac{dE_{halo}}{dN} = \Delta m c^2 - \langle E_\ell \rangle = m_D c^2 \left(\frac{\chi}{1 + \chi} - \gamma_D \frac{\chi(2 + \chi)}{2(1 + \chi)^2} \right) , \quad (10)$$

where N is the number of unstable particles. But the decay rate is

$$\frac{dN}{dt} = \frac{d}{dt} N_0 e^{-(t+t_f)/\tau} = -\frac{N_0}{\tau} e^{-(t+t_f)/\tau} , \quad (11)$$

where t_f is the time at which the halo forms, t is the time elapsed since the formation of the halo, τ is the mean lifetime of the parent particle D , and N_0 is the initial number of parent particles at the time the universe began its expansion. Combining these quantities, we can now find the rate at which the halo's energy changes with time:

$$\begin{aligned} \frac{dE}{dt} &= \frac{dE}{dN} \left| \frac{dN}{dt} \right| = \frac{(N_0 m_D) c^2}{\tau} e^{-(t+t_f)/\tau} \left(\frac{\chi}{1 + \chi} - \gamma_D \frac{\chi(2 + \chi)}{2(1 + \chi)^2} \right) \\ &= \frac{(M) c^2}{\tau} e^{-(t+t_f)/\tau} \left(\frac{\chi}{1 + \chi} - \gamma_D \frac{\chi(2 + \chi)}{2(1 + \chi)^2} \right) . \end{aligned} \quad (12)$$

By knowing the rate of energy change, we can in principle find the change in size of the halo by expanding it adiabatically. However, in order to do that, we need to know its initial density profile. At the time of formation, we will assume the halo has a Navarro, Frenk, & White density profile (1997, NFW hereafter)

$$\frac{\rho_{\text{NFW}}(r)}{\rho_{\text{crit}}} = \frac{\delta_\eta}{(r/r_s)(1 + r/r_s)^2} , \quad (13)$$

where ρ_{crit} is the critical density, r_s is the scale radius of the NFW profile, and

$$\delta_\eta = \frac{200}{3} \frac{\eta^3}{\ln(1 + \eta) - \eta/(1 + \eta)} \quad (14)$$

is a characteristic (dimensionless) density in terms of $\eta = r_v/r_s$ (the concentration parameter) and the virial radius r_v (defined as the radius of a sphere of mean interior density $200\rho_{\text{crit}}$). Although the NFW profile is an analytic function, it cannot be readily incorporated into our semi-analytical model. First, its distribution function $f(r, v)$ cannot be obtained analytically, and must be found numerically. Furthermore, to find how the scale radius r_s evolves with time, we need to find the halo energy as a function of r_s , but this is not easy to do with the NFW profile. Assuming the halo is virialized, $E_{\text{tot}} = \langle K \rangle + \langle U \rangle = -\frac{1}{2}\langle U \rangle + \langle U \rangle = \frac{1}{2}\langle U \rangle$. The total potential energy is given as (Binney & Tremaine 1987)

$$U = \frac{1}{2} \int \Phi(\mathbf{x})\rho(\mathbf{x}) d^3\mathbf{x} , \quad (15)$$

where Φ is the gravitational potential.

To evaluate this integral, we need to find $\Phi(\mathbf{x})$ from $\rho(\mathbf{x})$, which we can do by first finding the mass

$$M(r) = \int_0^r 4\pi r'^2 \rho(r') dr' . \quad (16)$$

For the NFW profile,

$$M_{\text{NFW}}(r) = M \frac{\ln(1 + r/r_s) - \frac{r/r_s}{1+r/r_s}}{\ln(1 + \eta) - \frac{\eta}{1+\eta}} , \quad (17)$$

where M is the virial mass of the halo contained inside the virial radius. By definition, $\nabla\Phi(\mathbf{x}) = -\mathbf{F}(\mathbf{x})$, and for the simple isotropic case, $\mathbf{F}(r) = -GM(r)/r^2$, which leads to

$$\Phi(r) = \int_0^r \frac{GM(r')}{r'^2} dr' . \quad (18)$$

For an NFW halo, this gives¹

$$\Phi_{\text{NFW}}(r) = \frac{-GM}{r} \frac{\ln(1 + r/r_s) - \frac{r/r_s}{(1+\eta)}}{\ln(1 + \eta) - \frac{\eta}{1+\eta}} . \quad (19)$$

Thus, solving for U in equation (15), we find that

$$E_{\text{NFW}} = -\frac{GM^2}{4r_s} \left(\frac{1 - 1/(1 + \eta)^2 - 2 \ln(1 + \eta)/(1 + \eta)}{[\ln(1 + \eta) - \eta/(1 + \eta)]^2} \right) . \quad (20)$$

In this equation, the concentration parameter η changes with r_s , which makes it difficult to find an analytic expression for dr_s/dt in terms of dE/dt .

For these reasons, it is convenient to translate the NFW profile into an equivalent Plummer

¹ To get the correct energy, the potential $\Phi(\mathbf{x})$ must be adjusted with an additive constant such that $\Phi(r_v) = -GM/r_v$, since the NFW halo density must vanish for $r > r_v$.

distribution,

$$\rho_p(r) = \left(\frac{3M}{4\pi r_p^3} \right) \left(1 + \frac{r^2}{r_p^2} \right)^{-5/2}, \quad (21)$$

which is mathematically easier to evolve in time. In this expression, r_p is the Plummer scale radius. A principal virtue of the Plummer profile is that it solves the Lane-Emden equation for a self-gravitating, polytropic gas sphere. The corresponding distribution function may be written

$$f_p(r, v) = B \left[\frac{GM}{\sqrt{r^2 + r_p^2}} - \frac{1}{2}v^2 \right]^{7/2}, \quad (22)$$

where B is a normalization constant, and it is trivial to show from equations (16) and (18) that

$$M_p(r) = M \frac{r^3}{(r_p^2 + r^2)^{(3/2)}}, \quad (23)$$

and

$$\Phi_p(r) = \frac{-GM}{\sqrt{r_p^2 + r^2}}. \quad (24)$$

Thus, the total energy of a Plummer halo (from equation 15) is

$$E_p = -\frac{3\pi GM^2}{64r_p}. \quad (25)$$

In making the transition from an NFW profile to its corresponding Plummer form, we use the physically reasonable criterion that two haloes should have the same mass and energy. Therefore, equating equations (20) and (25), we get

$$r_p = r_s \frac{3\pi}{16} \left(\frac{[\ln(1 + \eta) - \eta/(1 + \eta)]^2}{1 - 1/(1 + \eta)^2 - 2 \ln(1 + \eta)/(1 + \eta)} \right). \quad (26)$$

Following Navarro, Frenk, and White (1997), we will further assume that $\eta = 20$ at the time of formation (for the smallest haloes), though our results are insensitive to its actual value.

Figure 2 illustrates the differences in circular velocity ($v_{\text{circ}} = \sqrt{GM(r)/r}$) for an NFW halo (with mass $3 \times 10^8 M_\odot$) and the corresponding equivalent Plummer form. The Plummer halo may not fit the observed velocities as well as NFW, but their maximum circular velocities are almost the same, and since the Plummer model permits us to obtain an analytic solution for the halo's evolution in time, we will use it in all our calculations under the assumption that the collective behavior of self-gravitating virialized haloes is similar for slightly different profiles. Nevertheless, we will still need to use the NFW profile to obtain the initial characteristics of the halo at the time of its formation.

Now, using the Plummer distribution (equation 22), we can simplify equation (12) by evaluat-

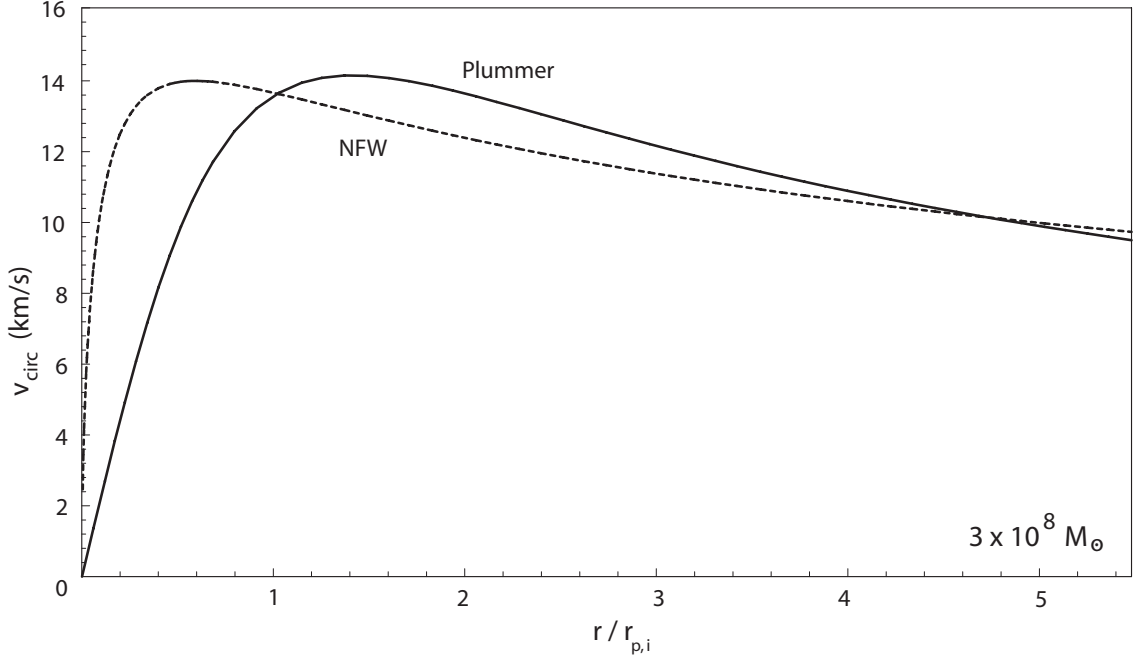


Figure 2. Circular velocity curves of two haloes with the same mass ($M = 3 \times 10^8 M_\odot$) and the same total internal energy, but one with a Plummer density profile, and the other with an NFW density profile. Radii are in units of the initial Plummer scale radius, $r_{p,i}$, and circular velocities in units of kilometers per second.

ing the average rate²

$$\begin{aligned} \left\langle \frac{dE}{dt} \right\rangle &= \int \frac{dE}{dt} f_p(r, v) d^3 \mathbf{x} d^3 \mathbf{v} \\ &= \frac{(M)c^2}{\tau} e^{-(t+t_f)/\tau} \left[\frac{\chi}{1+\chi} - \left(1 + \frac{3\pi GM}{64c^2 r_p} \right) \frac{\chi(2+\chi)}{2(1+\chi)^2} \right]. \end{aligned} \quad (27)$$

And combining equations (25) and (27), we therefore get

$$\begin{aligned} \frac{dr_p}{dt} &= \frac{64 r_p^2}{3\pi GM^2} \frac{dE}{dt} \\ &= \frac{64 r_p^2}{3\pi GM} \frac{c^2}{\tau} e^{-(t+t_f)/\tau} \left[\frac{\chi}{1+\chi} - \left(1 + \frac{3\pi GM}{64c^2 r_p} \right) \frac{\chi(2+\chi)}{2(1+\chi)^2} \right]. \end{aligned} \quad (28)$$

This differential equation can be solved analytically, yielding the result

$$r_p(t) = r_{p,i} \frac{3\pi GM(\chi+2) \exp\left[-\frac{\chi(\chi+2)}{2(\chi+1)^2} e^{-t_f/\tau}\right]}{64\chi c^2 r_{p,i} \exp\left[-\frac{\chi(\chi+2)}{2(\chi+1)^2} e^{-t_f/\tau}\right] + \left(3\pi GM(\chi+2) - 64\chi c^2 r_{p,i}\right) \exp\left[-\frac{\chi(\chi+2)}{2(\chi+1)^2} e^{-(t+t_f)/\tau}\right]}, \quad (29)$$

where $r_{p,i}$ is the initial Plummer scale radius at the time of formation. Note that the impact of DM decay on the evolution of the halo does not depend on the mass of the individual particles D and D' , but rather on the ratio of these masses represented by the unitless parameter χ , as well as on the mean lifetime τ of the parent particle D . There is an underlying assumption here that the halo

² Note that $\gamma_D = 1/\sqrt{1-v^2/c^2} \approx 1 + v^2/2c^2$ since particle D is non-relativistic.

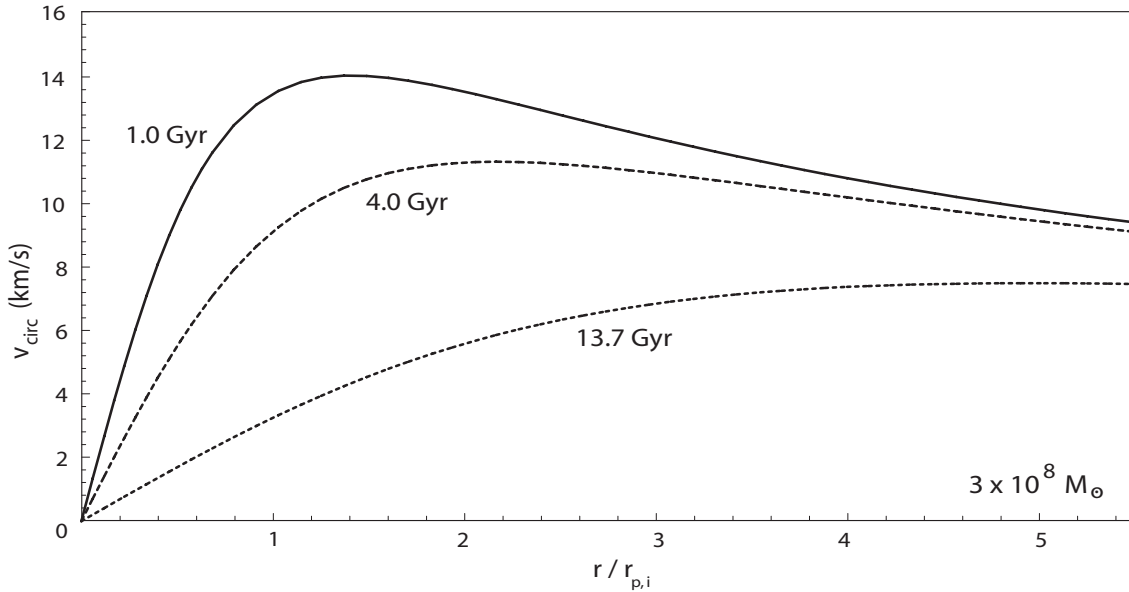


Figure 3. Circular velocity curves at different times (indicated) of an expanding halo formed at $t = 1 \text{ Gyr}$ with mass $3 \times 10^8 M_\odot$. The expansion is due to the decay of CDM particles with $\chi = 4 \times 10^{-5}$ and $\tau = 5 \text{ Gyr}$. The radius is in units of the initial Plummer scale radius, and circular velocities are km s^{-1} .

keeps a Plummer profile throughout the expansion. When comparing the decay time scale, defined as $t_{\text{decay}} \equiv |E/dE/dt|$, to the dynamical time $t_{\text{dyn}} \equiv \sqrt{3\pi/16G\rho}$ (Binney & Tremaine 1987), we find that $t_{\text{decay}}/t_{\text{dyn}} > 10$, implying that the halo always equilibrates to its virialized profile fast enough to justify the quasi-equilibrium approximation. Figure 3 illustrates the expansion of a halo formed at $t_f = 1 \text{ Gyr}$, showing how the maximum circular velocity decreases with time.

5 COMPUTATIONS AND RESULTS

To explore the global impact of our model on the halo distribution, we incorporate the effects of the DM decay on each individual halo (equation 29) and its formation rate (equation 2) through a series of calculations. We assess the consequences of this process by examining the modifications to the distribution of maximum circular velocity (v_{circ} hereafter) under two assumptions: (i) that at the time of formation, all haloes with the same mass will have the same concentration parameter. Although this is evidently incorrect for individual haloes, we are considering the global behavior, for which an average concentration parameter will suffice. Thus, in the case of no decay, all virialized haloes with the same mass will have the same circular velocity regardless of when they formed, since their concentration parameter does not change with time and only depends on the halo’s mass; (ii) that the stellar dispersion velocity is proportional to the maximum circular

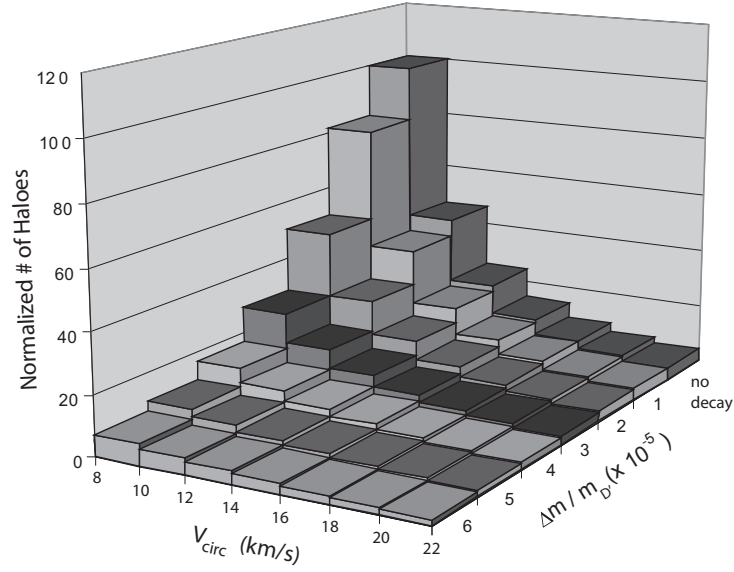


Figure 4. Circular velocity distribution of DM haloes for a fixed mean lifetime $\tau = 5$ Gyr, and different values of the decay parameter $\chi \equiv \Delta m / m_D$. The circular velocity distribution without decay is provided for comparison.

velocity of the host dwarf halo.³ Thus, with DM decay, the haloes expand and their concentration will correspondingly change with time, which in turn alters the circular velocity and the observed stellar dispersion velocity. So haloes with different masses that formed at different times in the past may end up with the same circular velocity in the current epoch.

For a given decay parameter χ and a mean lifetime τ , the evolution of the halo still depends on when it formed and on its mass. For example, if the halo formed late relative to the mean lifetime τ , then most of the unstable DM particles will have already decayed by then, and the halo will therefore experience no significant expansion. Furthermore, according to equations (12) and (25), $dE/dt \propto M$, while $E \propto M^2$, which means that $(dE/dt)/E \propto 1/M$. This is a crucial dependence of this process on mass since it guarantees a relatively stronger impact on the smaller haloes. For example, if a small halo with $M \approx 10^8 M_\odot$ experiences a significant expansion for a given set of decay parameters (for which, say, $(dE/dt)/E$ is of order unity), then a much larger halo, e.g., with $M \approx 10^{10} M_\odot$, will be unaffected by the decay since now $(dE/dt)/E \approx 10^{-2}$.

Figure 4 demonstrates the impact of changing the decay parameter χ on the circular-velocity distribution in the range 8–22 km s⁻¹, given a fixed mean lifetime. For this calculation, the forma-

³ This assumption has been extensively used to infer the circular velocity for elliptical galaxies and dwarf spheroidals from the observed stellar dispersion velocity $v_{\text{circ}} = \sqrt{3}\sigma$, where σ is the observed stellar dispersion velocity (Klypin et al. 1999, Simon & Geha 2007)

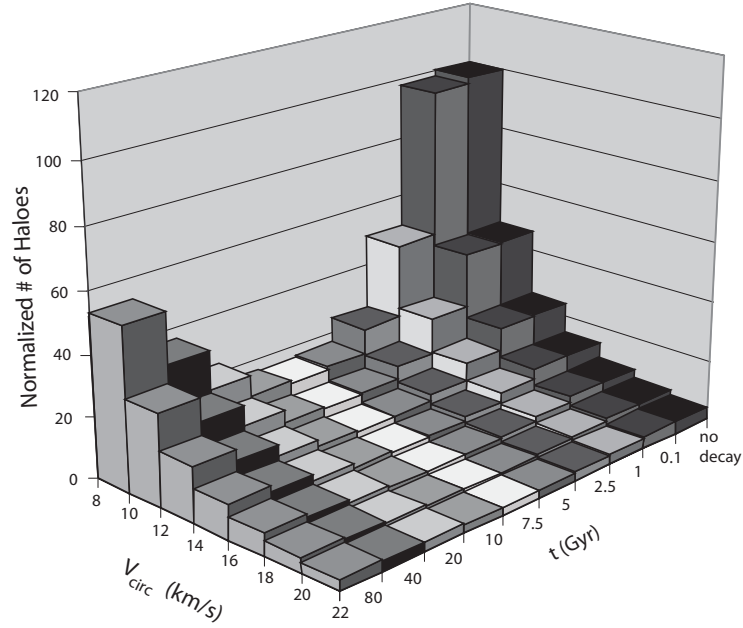


Figure 5. Circular velocity distribution of DM haloes for a fixed decay parameter $\chi = 4 \times 10^{-5}$, and different values of the mean lifetime τ . The circular velocity distribution without decay is provided for comparison.

tion time distribution function was normalized such that without any DM decay, 100 haloes would be produced with v_{circ} between 10 and 20 km s^{-1} . We can see that the decay decreases the number of haloes with lower circular velocities more than those with higher ones. Furthermore, the impact of the DM decay on the velocity distribution increases with χ , which is not surprising given that a higher χ corresponds to a higher recoil velocity of the remaining particle D' and, therefore, a greater expansion. It is important to note that our approximations cease to be valid at $\chi \approx 7 \times 10^{-5}$, because for higher values the recoil velocity of D' becomes comparable to its escape velocity in the haloes we are considering. For such high values of χ , some of the D' particles would start escaping right after the decay, depending on the velocity and initial position of the parent particle and on the angle θ^* that the recoil velocity makes with the velocity of the parent particle. As a result, the mass of the halo would decrease with time, an effect that is not being taken into account right now.

We have also examined the impact of varying the mean lifetime τ on our model, the results of which are summarized in figure 5, for a fixed value of χ . For relatively small values of τ (≈ 0.1 Gyr), the decay has virtually no impact on the circular velocity distribution since most of the DM particles will have already decayed before the vast majority of the haloes formed. In these cases,

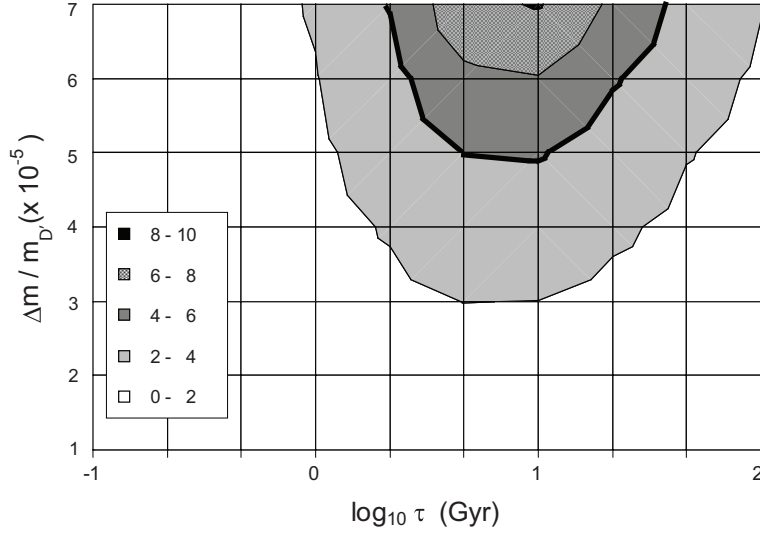


Figure 6. Contour plot representing the effectiveness of the DM decay in reducing the number of dwarf haloes with v_{circ} between 10 and 20 km s^{-1} , given a set of decay parameters $\chi \equiv \Delta m / m_D$ and τ . The shaded regions represent the ratio of the number of haloes predicted without decay (for v_{circ} between 10 and 20 km s^{-1}) to that obtained with DM decay.

the haloes experience no significant expansion. As τ increases, however, most of the DM particles decay after the majority of the haloes have formed.⁴ The impact of DM decay reaches a maximum ”effectiveness” in decreasing the number of haloes for $\tau \sim 10$ Gyr. As one would expect, larger values of τ produce less significant results since most of the unstable particles would not have decayed by the present time.

The full dependence of the circular-velocity distribution on DM decay is shown in figure 6, which includes the effects of both χ and τ . The contour levels represent the effectiveness of the decay in decreasing the number of dwarf haloes within the velocity range 10–20 km s^{-1} . The various shaded regions represent the expected number of haloes without decay divided by the corresponding number when expansion occurs with a given set of parameters χ and τ .

Besides adjusting the predicted circular velocity distribution to bring it in line with observations, the most important observational signature of DM decay is the dependence of the concentration parameter of dwarf galaxies on redshift. At relatively large redshifts, the haloes would have formed recently and a smaller fraction of the DM particles would have decayed, so neither the concentration parameter, nor the stellar dispersion velocity, would have been influenced greatly. This is to be contrasted with what would have happened to haloes observed in the current epoch. Therefore, distant dwarf haloes at large redshifts would be expected to be brighter (on average)

⁴ This implies that the dependence of our model on τ is strongly related to the formation time distribution function. Thus, using a different formation function can produce a qualitatively different dependence on τ .

and to have higher dispersion velocities compared to their nearby (lower redshift) counterparts with similar masses.

6 CONCLUSION

We have shown that the decay of unstable CDM particles can fully account for the deficit of dwarf galaxies in the local group, and have identified some of the particle properties required to achieve this result. In figure 6, the lifetime τ and energy conversion fraction χ must have values consistent with the thick black line between the two gray regions in order to reduce the number of dwarf haloes within the range of velocities 10–20 km s⁻¹ by a factor ~ 4 , in agreement with the observations (Simon & Geha 2007). Broadly speaking, the DM decay model works very well as long as $\chi \sim 5 - 7 \times 10^{-5}$. The lifetime cannot be longer than ~ 30 Gyr, and may be as short as only a few Gyr, depending on the precise value of χ . Note, however, that we have here restricted our analysis to cases in which the more massive decay particle D' remains bound to the halo. We may find other regions of $\chi - \tau$ phase space that produce reasonable results when this restriction is removed.

We emphasize that this model can reduce power on small scales consistent with the observations without altering the number of Milky Way-sized galaxies. Very importantly, we have shown that although the expansion produced by these decays changes the circular velocity distribution, it does not change the halo mass function, at least not directly. It is beyond the scope of the present paper to seek the ultimate fate of dwarf haloes expanding to circular velocities below 10 km s⁻¹, which remains an open question, though several possibilities have been proposed by Cen (2001a, 2001b).

It should be pointed out, however, that in addition to expanding (preferentially) the smaller haloes, and thereby reducing their measurable velocity dispersion, DM decay would also have the effect of speeding up their rate of evaporation within the Milky Way's tidal field. In this way, dwarf haloes would be removed from the overall velocity distribution, not only due to their migration in velocity space towards the low end, but would also be removed entirely due to evaporation. This effect would not be evident with the larger haloes, for which DM decay would have little impact on their condensation (and hence on their velocity profiles).

Interestingly, some limits on DM-decay models have already been established based on limits provided by the cosmic γ -ray background. Although it is beyond the scope of the present paper to consider the implications of our work on all possible DM scenarios, it is useful to see how coupling

our astrophysically-motivated simulations to the various particle physics proposals could develop in the future. For example, in their consideration of WIMPs decaying to Kaluza-Klein gravitons and gravitinos, Cembranos et al. (2007) demonstrated that both the energy spectrum and flux of the observed diffuse MeV γ -ray excess may be explained by decaying DM with \sim MeV mass splittings. In this picture, a decay timescale of 10 Gyr would require a mass splitting of \sim 10 MeV, for which the unstable DM particle would then have a mass \sim 1 TeV within the context of our model. In a second example, Kribs and Rothstein (1997) placed bounds on long-lived primordial relics using measurements of the diffuse γ -ray spectrum from EGRET and COMPTEL. They concluded that relics decaying predominantly through radiative channels are excluded for lifetimes between 10^5 and 10^{15} years. Since the DM decay timescale in our model fits within this range, the radiative decay of relics such as these could not resolve the dwarf spheroidal problem.

We have kept our analysis semi-analytical in order to better gauge the impact of our assumptions and chosen parameter values. Of course, to get a more accurate set of results, one should couple the properties of decaying DM particles with a more realistic N-body simulation. We intend to carry out such a calculation in the near future and will report the results elsewhere.

ACKNOWLEDGMENTS

This research was partially supported by NSF grant 0402502 at the University of Arizona, and a Miegunyah Fellowship at the University of Melbourne. We are very grateful to Romeel Davé for very helpful discussions. Part of this work was carried out at the Center for Particle Astrophysics and Cosmology in Paris.

REFERENCES

- Abadi, M. G., Navarro, J. F., Steinmetz, M., and Eke, V. R. 2003, *ApJ*, 597, 21
- Barkana, R. and Loeb, A. 1999, *ApJ*, 523, 54
- Belokurov, V. et al., 2007, *ApJ*, 654, 897
- Bennett, C. L., Halpern, M., Hinshaw, G., Jarosik, N., Kogut, A., Limon, M., Meyer, S. S. et al. 2003, *ApJS*, 148, 1
- Binney J. and Tremaine S. 1987, *Galactic Dynamics*, Princeton Univ. Press, Princeton
- Blitz, L., Spergel, D., Teuben, P., Hartmann, D., and Burton, W. B. 1999, *ApJ*, 574, 818
- Cembranos, J.A.R., Feng, J. L., and Strigari, L. E., 2007, *PRL*, 99, 191301
- Cen, R. 2001, *ApJ Letters*, 546, L77
- Cen, R. 2001, *ApJ Letters*, 549, L195
- Davis, M., Lecar, M., Pryor, C., and Witten, E. 1981, *ApJ*, 250, 423
- de Blok, W.J.G., Bosma, A., and McGaugh, S. 2003, *MNRAS*, 340, 657
- Dekel, A. and Piran, T. 1987, *ApJ Letters*, 315, L83
- Dekel, A. and Silk, J. 1986, *ApJ*, 303, 39
- Dicus, D. A. and Teplitz, V. L. 1986, *Phys. Rev. D*, 34, 934
- Diemand, J., Kuhlen, M., and Madau, P. 2007, *ApJ*, 657, 262
- Giraud, E. 2001, *ApJ Letters*, 558, L23
- Hennawi, J. F. and Ostriker, J. P. 2002, *ApJ*, 572, 41
- Kaplinghat, M., Knox, L., and Turner, M. 2000, *PRL*, 85, 3335
- Kitayama, T. and Suto, Y. 1996, *MNRAS*, 280, 638
- Kravtsov, A. V., Klypin, A. A., Bullock, J. S., Primack, J. R. 1998, *ApJ*, 502, 48
- Klypin, A., Kravtsov, A. V., and Valenzuela, O. 1999, *ApJ*, 522, 82
- Kribs, G. D., and Rothstein, I. Z., 1997, *Phys. Rev. D*, 55, 4435
- Mac Low, M.-M. and Ferrara, A. 1998, *ApJ*, 513, 142
- Melia, F. 2007, *MNRAS*, 382, 1917
- Melia, F. 2007, *New Astronomy*, submitted (arXiv:0711.4810v1)
- Moore, B., Ghigna, S., Governato, F., Lake, G., Quinn, T. et al. 1999, *ApJ Letters*, 524, L19
- Mould, J. R., Huchra, J. P., Freedman, W. L., Kennicutt, R. C., Ferrarese, L., Ford, H. C., Gibson, B. K. et al. 2000, *ApJ*, 529, 786
- Murali, C., Katz, N., Hernquist, L., Weinberg, D. H., Davé, R. 2002, *ApJ*, 571, 1
- Navarro, J. F., Frenk, C. S., and White, S.D.M. 1996, *ApJ*, 462, 563

- Perlmutter, S., Aldering, G., Goldhaber, G., Knop, R. A., Nugent, P., Castro, P. G., Deustua, S. et al. 1999, *ApJ*, 517, 565
- Press, W. H. and Schechter, P. 1974, *ApJ*, 187, 425
- Rees, M. J. 1986, *MNRAS*, 218, 25
- Riess, A. G., Filippenko, A. V., Challis, P., Clocchiatti, A., Diercks, A., Garnavich, P. M., Gilliland, R. L. et al. 1998, *AJ*, 116, 1009
- Sánchez-Salcedo, F. J. 2003, *ApJ Letters*, 591, L107
- Sasaki, S. 1994, *PASJ*, 46, 427
- Sciama, D. W. 1990, *ApJ*, 364, 549
- Simon, J. D., and Geha, M., 2007, *ApJ*, 670, 313
- Spergel, D. N. and Steinhardt, P. J. 2000, *PRL*, 84, 3760
- Spergel, D. N., Verde, L., Peiris, H. V., Komatsu, E., Nolta, M. R. et al. 2003, *ApJS*, 148, 175
- Springel, V., Frenk, C. S., and White, S.D.M. 2006, *Nature*, 440, 1137
- Turner, M. S. 1985, *Phys. Rev. D*, 31, 1212
- Turner, M. S., Steigman, G., and Krauss, L. M. 1984, *PRL*, 52, 2090